Internal Motility in Stiffening Actin-Myosin Networks

Jörg Uhde, Manfred Keller, and Erich Sackmann
Physik Department, Technische Universität München, D-85747 Garching, Germany

Andrea Parmeggiani[1,3] and Erwin Frey[1,2]
[1]*Hahn-Meitner-Institut, Abteilung Theorie, Glienicker Strasse 100, D-14109 Berlin, Germany*
[2]*Freie Universität Berlin, Physik, Arnimallee 14, D-14195 Berlin, Germany*
[3]*LDMIM, UMR 5539 CNRS/Université de Montpellier 2, 34095 Montpellier, France*
(Received 2 July 2003; published 20 December 2004)

We present a study on filamentous actin solutions containing heavy meromyosin subfragments of myosin II motor molecules. We focus on the viscoelastic phase behavior and internal dynamics of such networks during adenosine-triphosphate depletion. By combining microrheology and fluorescence microscopy, we observed a sol-gel transition accompanied by a sudden onset of directed filament motion. We interpret the sol-gel transition in terms of myosin II enzymology, and suggest a "zipping" mechanism to explain the filament motion in the vicinity of the sol-gel transition.

DOI: 10.1103/PhysRevLett.93.268101 PACS numbers: 87.16.Ka, 87.15.La, 87.15.Nn, 87.16.Nn

Eucaryotic cells show an amazing versatility in their mechanical properties. Not only can they sustain stresses ranging from some tenths to hundreds of Pascals, but they can equally well perform such complex processes as cytokinesis and cell locomotion. A vital role for these and other cellular functions is played by the cytoskeleton, the structural framework of the cell composed of a network of protein filaments. A major component is filamentous actin (F actin), whose physical properties are by now well characterized [1]. The length distribution, spatial arrangement, and connectivity of these filaments is controlled by a great variety of regulatory proteins.

An important family of these regulatory proteins are cross-linkers, which can be further classified as *passive* or *active*. The function of *passive cross-linkers*, e.g., α actinin, is mainly determined by their molecular structure and the on-off kinetics of their binding to actin. Upon changing the association-dissociation equilibrium and hence the degree of cross-linking by varying the temperature the network can be driven from a sol into a gel state [2]. Depending on both the concentration and the affinity of these cross-linkers for F actin there is a tendency to either form random networks or bundles [3]. Motor proteins of the myosin family can also act as *active cross-linkers*. When both of its functional head groups are bound to two different filaments they can use the energy of adenosine-triphosphate (ATP) hydrolysis to exert relative forces and motion between them. However, such an event is very unlikely under physiological conditions and ATP saturation, because then myosin II spends only a short fraction of its chemomechanical cycle attached to the filament (duty ratio: $r \lesssim 0.02$ [4]). Active relative transport yet becomes possible due to the concerted action of several motors if *in vitro* myosin II proteins assemble into multimeric minifilaments [5].

In this Letter we study actin networks containing the heavy meromyosin (HMM) subfragment lacking the light meromyosin domain responsible for myosin II assembly. Our focus is on the viscoelastic behavior and internal dynamics of such networks during ATP depletion. We use an experimental setup combining microrheology with fluorescent microscopy of labeled filaments. This allows us to identify a sol-gel transition accompanied by a sudden onset of directed filament motion.

Monomeric actin (G actin) was prepared from rabbit skeletal muscle as described previously [6]. To reduce residual cross-linking and capping proteins it was purified by an additional step using gel column chromatography (Sephacryl S-300). Actin was sterile filtered and kept in G buffer [6] on ice. Myosin II was obtained from rabbit skeletal muscle following Ref. [7]. HMM was prepared from this myosin II by chymotrypsin digestion following Ref. [8] with one modification: after the chymotrypsin treatment the solution was dialyzed against a large volume of low-salt buffer. The concentration was determined by absorption spectroscopy (absorption coefficient = 0.64 $\mathrm{cm}^2/\mathrm{mg}$ at 280 nm) [9]. HMM was stored either by rapid immersion of droplets in liquid nitrogen or by mixing with 30% sucrose. The frozen droplets or small aliquots of the mixed solution where stored at $-70\,^{\circ}\mathrm{C}$. Function tests for both myosin and HMM were performed by motility assays according to Ref. [10].

Fluorescently labeled reporter filaments were produced by polymerizing G actin (5 μM) in slightly modified F buffer ([6], using 0.2 mM ascorbic acid instead of dithiothreitole in the presence of equimolar tetramethylrhodamineisothiocyanate labeled phalloidin at room temperature. The reporter filaments were stored on ice and used within three days. The actin network was prepared in F buffer [6]. The ATP concentration was varied between 150 μM and 1 mM. An antioxidant (0.2 mg/mL glucose, 0.05 mg/mL glucose oxidase, 0.01 mg/mL catalase, 0.5 vol % mercaptoethanol) was added to the buffer solution. Samples where prepared by carefully mixing

1.5–3.0 μL of the fluorescently labeled reporter filaments to 0.5 mL of the buffer. After carefully mixing with HMM the polymerization was started by adding G actin. We used 200 μL of this solution for fluorescence microscopy measurements. The rest was carefully mixed with magnetic beads (Dynabeads M-450, Dynal, Hamburg, Germany; 4.5 μm radius) and used for magnetic tweezers experiments, as described in [11].

In our experiments we used freshly prepared actin kept on ice for at most 10 days. We worked with 9.5 and 19 μM solutions, corresponding to an actin concentration c_A of 0.4 and 0.8 mg/mL, equivalent to a mesh size $\xi \sim 0.5$ and $\sim$0.4 μm, respectively [12]. The ratio of labeled to unlabeled actin was between 1:300 and 1:1000. The molar ratios of actin-to HMM were $r_{AH} = 8, 12, 25, 50$, and 175, corresponding to HMM concentrations between 360 and 55 nM. After approximately 15–20 min, 90% of G actin is polymerized into F actin [13]. Measurements were started at least 5 min after polymerization was initiated. 80% of the reported filament transport events happened 15 min or later after the polymerization start.

Fluorescence measurements were performed in a closed sample chamber (containing approximately 100 μL) with an inverse microscope [Zeiss Axiovert 200, 100× oil immersion objective (N.A. 1.3)] and a charge-coupled device (CCD) camera (Orca C4742-95-12ER, Hamamatsu, Herrsching, Germany). 12 bit images of size 672×512 pixels (using 2×2 binning) were stored directly on a hard disk using the online image processing software "open box" [11]. The frame rate was approximately 17 Hz. A given region in the sample could be observed for several minutes before the contrast decreased significantly by photo bleaching.

We now discuss our results obtained with a magnetic tweezers microrheometer [11,14]. Magnetic beads of 4.5 μm diameter, embedded in the network during polymerization, were subjected to an oscillating magnetic force of $f = 1.5$–3 pN. Figure 1 shows the resulting oscillatory motion, analyzed by a particle tracking procedure with an accuracy better than 10 nm and time resolution less than 8 ms.

All our experiments show a characteristic time t_{sg}, where the bead amplitude starts to shrink. This is followed by a transition regime, $t_{sg} \leq t \leq t_g$, during which the bead amplitude falls below the noise level. We interpret this as a *sol-gel transition* caused by the continuous depletion of ATP. For $t \leq t_{sg}$, ATP is present in abundance resulting in a fast release of HMM from actin such that it cannot act as a cross-linker. The network exhibits the mechanical properties of a semidilute entangled solution of F actin. When ATP starts to lack, the residence time of HMM on actin increases, which in turn induces progressive cross-linking of the filaments leading to a stiffening of the network. In addition to their role as passive cross-linkers HMM also can actively generate forces between

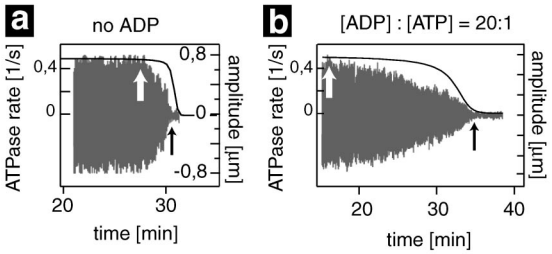

FIG. 1. Amplitudes of oscillating magnetic beads embedded in actin-HMM networks with no (a) and additional (b) initial ADP, showing transitions from a non–cross-linked F-actin solution to a gel state. The initial ATP concentration was 150 μM, $c_A = 9.5$ μM, $r_{AH} = 53$, $f = 2.55$ pN, and the oscillation frequency was 150 mHz. The solid lines show the calculated ATPase rate of a HMM (see text). Note that the time difference between t_{sg} (white arrows) and t_g (black arrows) increases with the ADP:ATP ratio. Increasing ATP concentration simultaneously shifts both t_{sg} and t_g to larger times (not shown).

filaments. These two different roles are not easily distinguished when looking at rheology data alone, but become evident from the dynamics of the embedded reporter filaments, which we discuss below.

Upon using known features of myosin II enzymology we can give an almost quantitative picture of the dynamics of the HMM molecules in the actin network and the resulting time dependence of the bead amplitudes during the process of ATP consumption. A rough estimate of the consumption rate is $k_c \simeq [\mathrm{ATP}]_0/[\mathrm{M}]_0 t_g$, where $[\mathrm{ATP}]_0$ is the initial ATP concentration and $[\mathrm{M}]_0$ is the total HMM concentration. This estimate neglects cooperative effects of preferential binding of HMM molecules close to already bound HMMs [15]. From the experimental data in Fig. 1 one gets $k_c \approx 0.4\ \mathrm{s}^{-1}$ for each HMM, which is much closer to the ATPase rate in the absence of actin than in a saturated F-actin solution [4]. We explain this as a consequence of the diffusive search of the HMM for an actin filament being the rate limiting process. The characteristic rate of search and binding to an actin filament can be estimated as $k_s \sim k_d \phi$, where $k_d \simeq 6D\xi^{-2}$ is the rate for diffusing a distance comparable to the mesh size ξ; D is the diffusion constant of HMM in water and ϕ is the volume fraction of actin in solution. From experimental data we estimate [16] $k_s \sim 0.37\ \mathrm{s}^{-1}$ which is quite close to the experimental value of $0.45\ \mathrm{s}^{-1}$.

Starting from these considerations we calculated the ATP consumption rate as a function of time using known rates from the literature [18] with the exception of k_s, which was computed along the lines explained above. The results are shown as the solid line in Fig. 1. The sol-gel transition starts at a time t_{sg} when ATP depletion becomes significant and the typical ATPase rate starts to decrease. Note that we have to account for the inhibition effect of adenosine-diphosphate (ADP), which increases

with time because of the ATP hydrolysis. ADP plays an important role both for the shape of the ATPase rate and the estimates of t_{sg} and t_g. An increase of the initial ADP concentration decreases t_{sg} while it increases t_g, thus increasing the time window t_g-t_{sg} [19] (cf. Fig. 1). The model we used to compute the ATPase rate shows that the fraction of bound HMM increases with ADP content [19]. Therefore the onset of gelation at t_{sg} occurs earlier due to the increase of bound HMM, whereas the ATPase rate is slowed down and t_g is shifted to longer times.

Our experimental setup allows us to simultaneously measure the amplitude of embedded beads and the dynamics of fluorescently labeled reporter filaments. At the beginning of the experiment, when the network is still not fully polymerized, these filaments diffuse freely as in bulk solutions. Towards the end of the polymerization process when $t \leq t_{sg}$, the movement of the reporter filaments becomes more and more restricted by the surrounding network. The filaments show thermal undulations and perform Brownian motion along the cylindrical cages formed by the surrounding F actin. In contrast to an actin network containing myosin II minifilaments [5], here long distance directed motion of F actin is observed only very rarely. During the sol-gel transition, $t_{sg} \leq t \leq t_g$, any drift that sometimes was observed in the sample chamber came to a rather abrupt end indicating the stiffening of the network. At the same time single filaments that shortly before had hardly shown any fluctuations, suddenly started long term directed motion inside the three-dimensional network [Figs. 2(a)–2(c)].

In our study, 132 moving filaments were evaluated. The phenomenon of moving filaments in the actin-HMM network occurs in a narrow time slot of some minutes upon approaching the gelation point t_g while there are also some rare events of directed filament motion outside this time window. Within such time window up to 40% of the filaments in focus move. The phenomenon occurs under different buffer conditions, different actin and HMM concentrations, and different molar actin-to-HMM ratios. Since aging of HMM is affecting the motion, only experiments performed on the same day with the same actin preparation and HMM stock solution were compared.

The values obtained for the filament mean run length and mean velocity are compatible with two dimensional motility assays at low ATP concentration [4]. The continuous longitudinal motion occurred at speeds up to 2.6 μm/s over distances up to 37 μm and for times up to 100 s. The movement consists of an acceleration phase, a phase of constant speed, and a deceleration phase [cf. Fig. 2(c)]. Because of experimental limitations, not all the observed filaments could be monitored in all three phases.

In our experiments we observed a broad distribution of run lengths. As a general tendency, long filaments

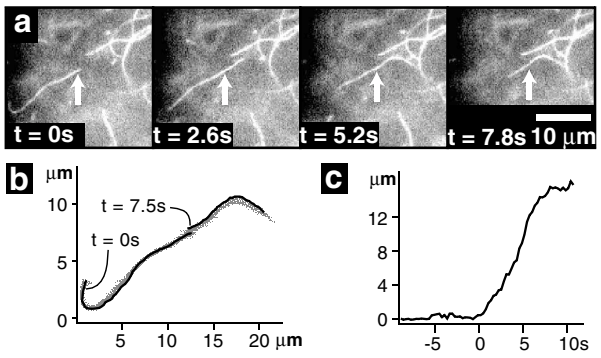

FIG. 2. Sequence of fluorescence micrographs showing the movement of an actin filament in the actin-HMM network with $c_A = 9.5$ μM ($\xi \sim 0.5$ μm) and $r_{AH} = 12$. Note that the leading end of the filament is moving out of focus. (a) The time sequence shows a reporter filament of length 16.5 μm (indicated by arrows), which within 8 s moves over a distance of 16.5 μm at an average speed of 2 μm/s. (b) Superposition of 69 traced contours. Traces corresponding to the reporter filament before ($t = 0$ s) and after ($t = 7.8$ s) active transport are shown explicitly. (c) Time evolution of the filament position along its average contour. Note the sudden onset at $t = 0$ s and halt at $t = 8$ s.

(>15 μm) moved distances up to their own visible length and then paused, while some short filaments (< 5 μm) ran out of focus over distances even larger than 5 times their own visible length [17]. Figure 2 shows a long filament which moves about its own visible length.

We interpret the sudden onset of directed filament motion in the vicinity of the sol-gel transition as follows. In a three-dimensional actin network double-headed myosin can exert forces between filaments only if its heads are simultaneously attached to two different filaments while one of its heads is performing a power stroke. Since under saturating ATP condition myosin II has a very low duty ratio, such events are extremely rare. Actin filaments can be transported only if a certain number of motors work together as in the thick filament of a sarcomere. A similar effect seems to be at work in recent experiments where myosin II molecules arrange themselves into minifilaments [5]. In the present study we use HMM, which does not form such minifilaments. Hence cooperativity of the motors must be achieved by a different route. Since ATP is needed to trigger the dissociation of the motor from the filament and since its concentration is continuously reduced due to motor-induced hydrolysis, the time a myosin head stays bound to a filament (duty ratio) is prolonged. This increases the probability for the other head to also bind to a filament while the first one is still bound. As a consequence, one can have two opposing effects. First, an increasing fraction of HMM molecules acts as cross-linkers in the actin network, and stiffens it. This explains the sol-gel transition observed by the sudden decrease in the amplitude of the oscillating magnetic bead (cf. Fig. 1), and also the stop of a drift in the sample

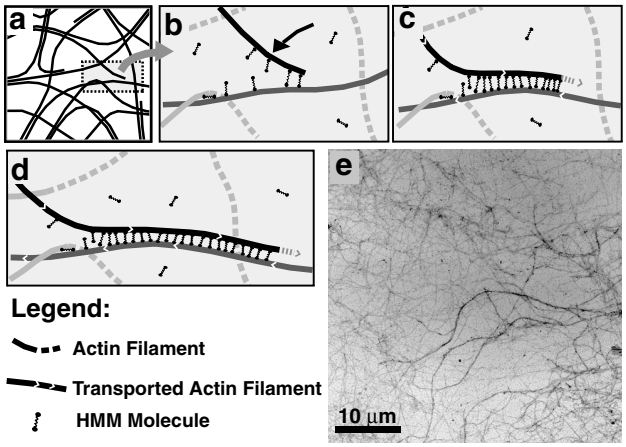

FIG. 3. (a)–(d) Illustration of the zipping mechanism (see main text). (e) Electron micrograph of the network in the vicinity of the sol-gel-transition showing the formation of entangled actin bundles.

chamber as mentioned above. Second, the probability that myosin molecules can exert directed forces onto actin filaments is also increased.

One may envisage a *zipping mechanism* as illustrated in Figs. 3(a)–3(d). After the two heads of a HMM molecule happen to bind two antiparallel filaments simultaneously, thermal fluctuations in the vicinity of the binding site are reduced. This enhances the probability that nearby myosin also bind to both filaments and leads to a nucleation process which zips the filaments together and generates relative filament motion. Single filaments may also slide along bundles generated during the zipping or the gelation process. During the transport the overlap region grows, which explains the sudden onset of filament motion and the moderate acceleration phase (cf. Fig. 2).

Note that a moderate increase of rigor bonds favors zipping but does not impede filament motion since the ADP-HMM–actin bonds are strongly weakened by tangential forces of the order of 10 pN [20,21]. Therefore motility stops only if the population of rigor states becomes much larger then the population of active motors.

We have explored how the observed effects depend on actin, c_A, and HMM concentration, c_H, and found the following tendencies. Doubling c_A from 9.5 to 19 μM while keeping $c_H = 0.38$ μM constant reduces the average transport length by a factor of 3. This is most likely due to the combined effect of a lowered number of motors per unit length on the filaments and the reduced mesh size. The latter enhances molecular crowding and reduces run length because of entanglement and unzipping effects.

Reducing c_H from 1.05 to 0.38 μM (with $c_A = 9.5$ μM fixed) lowers the average transport speed from 0.5 to 0.31 μm/s. This may be understood as a result of the reduced number of motors in the zipped region between the filaments. In general, we observe large variations in run length, time, and speed. For a given filament length the run length and average speed typically varied by factors 4 and 10, respectively. This may be due to heterogeneities in the network [see Fig. 3(e)], length distribution of actin filaments, their relative orientation [22] as well as the location of the initial seed in the zipping process, since only the reporter filaments could be observed. Future experiments with a much larger number of traced filaments and samples and the visualization of all filaments involved in the motility are certainly necessary to explore the details of this fascinating dynamic phenomenon.

We thank H. Kirpal for HMM preparations, M. Rusp for actin preparations and her help with the electron microscope, and J. Schilling for providing the "open box" software. We acknowledge financial support by the DFG (SFB 413) and the Fonds der Chemischen Industrie. A. P. was supported by a Marie-Curie grant under Contract No. HPMF-CT-2002-01529. We have profited from discussions with K. Kroy and G. Lattanzi.

[1] L. LeGoff *et al.*, Phys. Rev. Lett. **89**, 258101 (2002).
[2] M. Tempel *et al.*, Phys. Rev. E **54**, 1802 (1996).
[3] D. Wachsstock *et al.*, Biophys. J. **65**, 205 (1993).
[4] J. Howard, *Mechanics of Motor Proteins and the Cytoskeleton* (Sinauer Associates, Sunderland, MA, 2001).
[5] D. Humphrey *et al.*, Nature (London) **416**, 413 (2002).
[6] J. A. Spudich and S. Watt, J. Biol. Chem. **246**, 4866 (1971).
[7] S. S. Margossian and S. Lowey, Methods Enzymol. **85**, 55 (1982).
[8] S. J. Kron *et al.*, Methods Enzymol. **196**, 399 (1991).
[9] A. G. Weeds and B. Pope, J. Mol. Biol. **111**, 129 (1977).
[10] S. J. Kron and J. A. Spudich, Proc. Nat. Acad. Sci. U.S.A. **83**, 6272 (1986).
[11] M. Keller *et al.*, Rev. Sci. Instrum. **72**, 3626 (2001).
[12] C. F. Schmidt *et al.*, Macromolecules **22**, 3638 (1989).
[13] P. Detmers *et al.*, J. Biol. Chem. **256**, 99 (1981).
[14] F. G. Schmidt *et al.*, Eur. Biophys. J. **24**, 348 (1996).
[15] A. Orlova and E. Egelman, J. Mol. Biol. **265**, 469 (1997).
[16] For the estimate we take the Einstein-Stokes relation $D = k_B T/6\pi\eta_w r$, where $\eta_w = 10^{-3}$ kg/(m s), $k_B T = 4 \times 10^{-21}$ J, and the hydrodynamic radius of HMM is $r \sim 15$ nm. Our estimate for the volume fraction is $\phi \sim 0.1\%$ within an uncertainty of 30% [17].
[17] M. Keller, Ph.D. thesis, TU München, 2003.
[18] We use the enzymatic rates of Table 14.2 in Ref. [4]. A detailed analysis and study of the inhibition effect of ADP will be published in a more extended article [19].
[19] M. Keller, A. Parmeggiani, E. Sackmann, and E. Frey (unpublished).
[20] T. Nishizaka *et al.*, Biophys. J. **79**, 962 (2000).
[21] A. Parmeggiani *et al.*, Europhys. Lett. **56**, 603 (2001).
[22] K. Kruse and F. Jülicher, Phys. Rev. Lett. **85**, 1778 (2000)